Velocity analysis using nonhyperbolic moveout in transversely isotropic media

Tariq Alkhalifah
Center for Wave Phenomena
Colorado School of Mines

ABSTRACT

P-wave reflections from horizontal interfaces in transversely isotropic (TI) media have nonhyperbolic moveout. Alkhalifah and Tsvankin (1995) showed that such moveout as well as all time-related processing in TI media with a vertical symmetry axis (VTI media) depend on only two parameters, called $V_{\rm nmo}$ and η. They also showed that these two parameters can be estimated from the P-wave dip-moveout behavior of surface seismic data.

Alternatively, one could use the nonhyperbolic moveout for parameter estimation. The quality of resulting estimates depends largely on the departure of the moveout from hyperbolic and its sensitivity to the estimated parameters. The size of the nonhyperbolic moveout in TI media is primarily dependent on the anisotropy parameter η. An "effective" version of this parameter provides a useful measure of the nonhyperbolic moveout even in isotropic $v(z)$ media. Moreover, effective η, $\eta_{\rm eff}$, is used to show that nonhyperbolic moveout associated with typical TI media (e.g., shales, with $\eta \simeq 0.1$) is larger than that associated with typical $v(z)$ isotropic media. The departure of moveout from hyperbolic is increased when typical anisotropy is combined with vertical inhomogeneity.

The stability of the nonhyperbolic-moveout inversion depends largely on the range of offsets used in the inversion procedure. Larger offset-to-depth ratios (X/D) provide more nonhyperbolic information, and therefore, increased stability and resolution in the inversion. The X/D values (e.g., $X/D > 1.5$) needed for obtaining stability and resolution are within conventional acquisition limits, especially for early zero-offset times.

Although estimation of η using nonhyperbolic moveouts is not as stable as that by the dip-moveout method of Alkhalifah and Tsvankin (1995), particularly in the absence of large offsets, it does offer some flexibility: it can be applied in the absence of dipping reflectors and may also be used to estimate lateral η variations. Application of the nonhyperbolic inversion to data from offshore Africa demonstrates its usefulness, especially in estimating lateral and vertical variations in η.

Key words: transverse isotropy, nonhyperbolic moveout, velocity analysis

Introduction

Often, the earth's subsurface is dominated by interfaces that are horizontal or sub-horizontal. Therefore, reflections from such interfaces are the primary source of information in much seismic data. Moveout from sub-horizontal reflectors, for example, provides useful velocity information. Fortunately, reflection moveouts from horizontal interfaces are generally well represented by truncated Taylor's series-type characterizations of moveout in transversely isotropic (TI) media with vertical symmetry axis (Hake et al., 1984; Tsvankin and Thom-

sen, 1994). These representations are accurate to and beyond the large offsets often used in practice.

Alkhalifah and Tsvankin (1995) demonstrated that, for TI media with vertical symmetry axis (VTI media), just two parameters are sufficient for performing all time-related processing, such as normal moveout (NMO) correction (including non-hyperbolic moveout correction, if necessary), dip-moveout (DMO) correction, and prestack and poststack time migration. Taking V_h to be the P-wave velocity in the horizontal direction, the two anisotropy parameters are

$$\eta \equiv 0.5(\frac{V_h^2}{V_{\rm nmo}^2} - 1) = \frac{\epsilon - \delta}{1 + 2\delta}\,, \tag{1}$$

and the short-spread NMO velocity for a horizontal reflector

$$V_{\rm nmo} = V_{P0}\sqrt{1 + 2\delta}\,. \tag{2}$$

Here, V_{P0} is the P-wave vertical velocity, and ϵ and δ are two of Thomsen's (1986) dimensionless anisotropy parameters.

Moreover, Alkhalifah and Tsvankin (1995) show that these two parameters, η and $V_{\rm nmo}$, are obtainable solely from surface seismic P-wave data, specifically from estimates of stacking velocity for reflections from interfaces having two distinct dips (the DMO method). The two-parameter representation and inversion also holds in $v(z)$ media. Alkhalifah (1996b) used the DMO inversion method to invert for vertical variations in η. However, the DMO inversion of Alkhalifah and Tsvankin (1995) and Alkhalifah (1996b) works only when reflectors with at least two distinct dips (e.g., a fault and a gently dipping reflector) are present, as long as one of the dips is not close to 90 degrees.

Hake et al. (1984) derived the three-term Taylor's series expansion of the reflection moveout from horizontal reflectors in VTI media. The presence of the third term in their expansion implies nonhyperbolic moveout. Tsvankin and Thomsen (1994) recast the three-term expansion as a function of Thomsen's (1986) parameters, which provided a more compact equation. Moreover, using an asymptotic fit, Tsvankin and Thomsen suggested a correction factor that approximates the deleted higher-order terms of the Taylor's series expansion, thus stabilizing the moveout at long offsets. Tsvankin and Thomsen (1995) studied the problem of inverting for Thomsen's anisotropy parameters (V_{P0}, ϵ and δ) using the nonhyperbolic moveout of reflections from horizontal interfaces. They found that such an inversion using only P-wave data would be highly ill-conditioned because of the trade-off between the vertical velocity and anisotropic coefficients, which cannot be overcome by using even twice the spread-to-depth length, which is in agreement with the two-parameter dependency of time-related processing (Alkhalifah and Tsvankin, 1995). They also point to the ambiguity in resolving the second-(A_2) and fourth order (A_4) coefficients of the Taylor's series expansion using traveltime moveout for ray angles up to 45 degrees. Although such ambiguity exists in the general sense of using traveltimes to invert for A_2 and A_4, it can be somewhat overcome by extracting A_2, which is simply the reciprocal of the NMO velocity squared, from conventional velocity semblance analysis, and in turn using it in the inversion for A_4, or in my case η. In fact, as we will see later, a 2-D semblance scan over both parameters proves to be a reliable method. Neidell and Taner (1971) have stated the clear benefits of semblance analysis for parameter extraction.

Byun et al. (1989) applied a two-parameter velocity analysis on synthetic vertical-seismic-profile (VSP) data using a "skewed" hyperbolic moveout formula for horizontal reflectors. Although their velocity-analysis approach showed promise, their nonhyperbolic (or skewed hyperbolic) formula was a coarse approximation to the actual moveout in TI media (Tsvankin and Thomsen, 1994). For example, their formula required knowledge of the vertical P-and S-wave velocities, whereas the true moveout is very much independent of these two parameters (Alkhalifah and Tsvankin, 1995).

Use of the deviation of moveout from hyperbolic for parameter estimation in general depends on the size of the deviations, as well as, on the sensitivity of the nonhyperbolic moveout to the estimated parameters and the absence of complicating factors such as lateral velocity variation. Here, I compare the size of nonhyperbolic moveout reflections from horizontal interfaces in VTI media with those associated with typical vertically inhomogeneous isotropic media. Then, I invert for estimates of η using the nonhyperbolic moveout, and discuss the sensitivity of the inversion to errors in the measured parameters, namely $V_{\rm nmo}$ and traveltime. I also apply semblance analyses over nonhyperbolic trajectories to estimate both $V_{\rm nmo}$ and η. The study includes field data applications that exemplify the usefulness of this method.

Nonhyperbolic Moveout in Layered Media

Hake et al. (1984) derived a three-term Taylor's series expansion for the moveout of reflections from horizontal interfaces in homogeneous, VTI media. If we ignore the contribution of the vertical shear-wave velocity, V_{S0}, which is negligible (Tsvankin and Thomsen, 1994; Alkhalifah and Larner, 1994; Tsvankin, 1995; Alkhalifah, 1996c), their equation can be simplified when expressed in terms of η and $V_{\rm nmo}$, as follows:

$$t^2(X) = t_0^2 + \frac{X^2}{V_{\rm nmo}^2} - \frac{2\eta X^4}{t_0^2 V_{\rm nmo}^4}. \quad (3)$$

Here, t is the total travel time, t_0 is the two-way zero-offset traveltime, and X is the offset. The first two terms on the right correspond to the hyperbolic portion of the moveout, whereas the third term approximates the non-hyperbolic contribution. Note that the third term (fourth-order in X) is proportional to the anisotropy parameter η, which therefore controls nonhyperbolic moveout directly.

Tsvankin and Thomsen (1995) derived a correction factor to the nonhyperbolic term of Hake et al. (1984) equation that increases the accuracy and stabilizes traveltime moveout at large offsets in VTI media. The more accurate moveout equation, when expressed in terms of η and $V_{\rm nmo}$ is given by

$$t^2(X) = t_0^2 + \frac{X^2}{V_{\rm nmo}^2} + \frac{2\eta X^4}{t_0^2 V_{\rm nmo}^4 (1 + AX^2)}, \quad (4)$$

where

$$A = \frac{2\eta}{t_0^2 V_{\rm nmo}^4 (\frac{1}{V_h^2} - \frac{1}{V_{\rm nmo}^2})},$$

and the horizontal velocity, V_h, from equation (1) for homogeneous media, is given by

$$V_h = V_{\rm nmo}\sqrt{1 + 2\eta}.$$

Through simple manipulation, equation (4) reduces to

$$t^2(X) = t_0^2 + \frac{X^2}{V_{\rm nmo}^2} - \frac{2\eta X^4}{V_{\rm nmo}^2[t_0^2 V_{\rm nmo}^2 + (1 + 2\eta)X^2]} \quad (5)$$

(Alkhalifah and Tsvankin, 1995). The difference between equations (4) and (5) will become evident in the $v(z)$ case, where V_h will be defined in two different ways. Equation (5) is accurate for large offset-to-depth ratios. Note that, by setting $X = 0$ in the denominator of the fourth-order term, equation (5) reduces to equation (3). The additional X factor in the denominator produces an expansion that approximates the influence of the terms (beyond the fourth-order) that were omitted in the Taylor's series expansion, and therefore increases the moveout accuracy at large offset. The higher-order approximation is based on the fact that as X becomes very large (goes to infinity), while t_0 is finite, equation (5) reduces to

$$t^2(X) = \frac{X^2}{V_h^2}. \quad (6)$$

Therefore, equation (6) is asymptotically exact, because the ray path in this case is horizontal.

Equations (3) and (4) can be used as well in layered media, with a small-offset approximation of the type made by Dix (1955). Hake et al. (1984) and Tsvankin and Thomsen (1994) provided key equations for moveout in layered VTI media, but in terms of conventional elastic coefficients and Thomsen's (1986) parameters, respectively. Here, I recast their expressions in terms of the practical anisotropy parameters η and $V_{\rm nmo}$.

First, as usual, the normal-moveout velocity involves a root-mean-squared (rms) average of velocities in the previous layers. Specifically

$$V_{\rm nmo}^2(t_0) = \frac{1}{t_0}\int_0^{t_0} v_{\rm nmo}^2(\tau)d\tau, \quad (7)$$

where all lower-case variables V, including $v_{\rm nmo}$, correspond to interval-velocity values, and the integration is over time for the vertical raypath. Therefore, $v_{\rm nmo}$ is the interval NMO velocity given by

$$v_{\rm nmo}(\tau) = v(\tau)\sqrt{1 + 2\delta(\tau)},$$

and $v(\tau)$ is interval vertical velocity. On the other hand, upper-case variables V, including $V_{\rm nmo}$, correspond to quantities that are averages for the entire vertical column from the surface to the reflector of interest. (Recall, here $V_{\rm nmo}$ refers to the NMO velocity for *horizontal* or near horizontal reflectors.)

Next, starting with Tsvankin and Thomsen's expansion for the coefficient of the fourth-order term in Hake's equation for moveout in layered VTI media, in Appendix A I find that equations (3) and (4) continue to hold, with η replaced by

$$\eta_{\rm eff}(t_0) = \frac{1}{8}\{\frac{1}{t_0 V_{\rm nmo}^4(t_0)}\int_0^{t_0} v_{\rm nmo}^4(\tau)[1+8\eta(\tau)]d\tau - 1\}. \quad (8)$$

Here, $\eta(\tau)$ is the instantaneous value of the anisotropy parameter η as a function of the vertical reflection time. In homogeneous isotropic media [$\eta(\tau) = 0$], expressions (7) and (8) inserted into equation (3) reduce to the familiar three-term expansion given by Taner and Koehler (1969), as shown in Appendix B. Now, in equation (4) Tsvankin and Thomsen (1994) suggested that V_h be computed using the following rms relation

$$V_h^2(t_0) = \frac{1}{t_0}\int_0^{t_0} v_h^2(\tau)d\tau, \quad (9)$$

where

$$v_h(\tau) = v_{\rm nmo}(\tau)\sqrt{1 + 2\eta(\tau)}.$$

Note that, in this case, equation (4) is described by three effective parameters ($V_{\rm nmo}$, V_h, and $\eta_{\rm eff}$). This would complicate velocity analysis and inversion applications requiring, among other things, three-parameter searches. On the other hand, a slightly different definition of V_h, given by

$$V_h(t_0) = V_{\rm nmo}(t_0)\sqrt{1 + 2\eta_{\rm eff}(t_0)}, \quad (10)$$

will reduce the number of effective parameters to two ($V_{\rm nmo}$ and $\eta_{\rm eff}$), simplifying the equation for later uses. In this case, equation (5) holds for layered media with η replaced by $\eta_{\rm eff}$, which is computed using equation (8).

The right side of Figure 1 shows the percent error in the computed moveout corresponding to reflections from (a) the bottom of the second layer, and (b) the bottom of the third layer in the model shown on the left side of the figure. Clearly, for $X/D < 2$, the moveout corresponding to $\eta_{\rm eff}$, calculated using equation (5) (gray curve) has smaller error (better approximates the exact moveout) than does the moveout corresponding to equation (4), using V_h calculated from equation (9) (black curve). Both approximations give better results than does moveout described by equation (3) (dashed curve), modified from Hake et al. (1984). $V_{\rm nmo}$ for all three approximate curves is the same, and is calculated using equation (7). Therefore, not only did the modified V_h expression (10) simplify the problem by reducing the number of required effective parameters, it apparently provided a better approximation to the exact moveout. Although only one example is shown here, this conclusion holds for many other $v(z)$ VTI models tested.

A definition of V_h that is more in line with the asymptotic approximation used to produce equation (4) is to take V_h as the maximum horizontal velocity among the overlaying layers. Such a definition of V_h, however, is not practical for typical seismic spreads because, although the definition is accurate asymptotically, it can considerably overestimate V_h at practical offsets (e.g., for models that include a thin layer with a high v_h).

Isotropic media are simply a subset of VTI media, where ϵ and δ equal zero [$\eta(\tau)$=0]. Therefore, equations (3) and (5) can be used to approximate moveout in isotropic layered media. Thus, although the anisotropy parameter $\eta(\tau)$ equals zero throughout, because the medium is inhomogeneous, $\eta_{\rm eff}(t_0)$, as given by equation (8), is nonzero. In fact, equation (3) reduces to the familiar three-term expression given by Taner and Koehler (1969) for isotropic media (see Appendix B). Therefore, the value of $\eta_{\rm eff}$ can as well be used to describe the departure from hyperbolic moveout caused by the inhomogeneity, in isotropic layered media, above a certain reflector. For isotropic $v(z)$ media, equation (4) yields hyperbolic moveout using Tsvankin and Thomsen's definition of V_h [equation (9)], and therefore ignoring nonhyperbolic moveouts associated vertical inhomogeneity. Better estimates of the moveout are achieved by using the new definition of V_h [equation (10)]. However, for isotropic media, the nonhyperbolic moveout given by equation (5) becomes slightly less accurate than that in equation (3) (see Appendix B). The reason for the reduced accuracy is that the correction factor introduced by Tsvankin and Thomsen is based on the anisotropy assumption only. Therefore, although it produces highly accurate moveout description for homogeneous VTI media, equation (5) has increased errors when inhomogeneity is introduced to the model (Appendix B). Fortunately, the errors arising from using equation (5) for all models shown (using examples with strong vertical inhomogeneity) are nevertheless less than 0.5% for X/D <2, rather independent of the strength of anisotropy.

Properties of the Nonhyperbolic Moveout

From equations (3) and (5), the value of $\eta_{\rm eff}$ for a given $V_{\rm nmo}$ and t_0 directly describes the degree of nonhyperbolic moveout in both anisotropic and isotropic layered media. For $\eta_{\rm eff}$=0, the fourth-order term in equation (5) vanishes, and the moveout is hyperbolic. This is the case in homogeneous isotropic or elliptically isotropic media.

Referring to Figure 1, one cannot distinguish between the amount of nonhyperbolic moveout due to anisotropy and that due to inhomogeneity. If this medium, with its large vertical inhomogeneity, were strictly isotropic (ϵ=0 and δ=0 in each layer) then $\eta_{\rm eff}$, calculated using equation (8), would equal 0.06. In contrast, the presence of anisotropy resulted in $\eta_{\rm eff}$=0.19. The difference between the two $\eta_{\rm eff}$ values, however, is not directly attributable to anisotropy because the relation between these factors is nonlinear.

The value of 0.06 for $\eta_{\rm eff}$ in this three-layer example results from a strong vertical inhomogeneity. I find $\eta_{\rm eff}$ values associated with more typical $v(z)$ (average gradient of 0.6 s^{-1}) isotropic media to be much smaller than 0.1, a common value for typical TI media; thus, nonhyperbolic moveout is less severe for typical isotropic $v(z)$ media than for common homogeneous VTI media. For example, let us approximate the velocity increase with depth in an isotropic medium [$\eta(\tau) = 0$] by a constant velocity gradient, a, with v_0 as the velocity at the surface; that is,

$$v(z) = v_0 + az.$$

For such a medium, velocity can be expressed in terms of two-way vertical traveltime, t_0 as

$$v(t_0) = v_0 e^{0.5\, a\, t_0}.$$

Through straightforward derivation using equations (7) and (9), we find that for such a constant-gradient medium,

$$\eta_{\rm eff}(t_0) = \frac{1}{8}\left(\frac{0.5\, a\, t_0}{\tanh(0.5\, a\, t_0)} - 1\right). \qquad (11)$$

Here, tanh is the hyperbolic tangent function. Note that

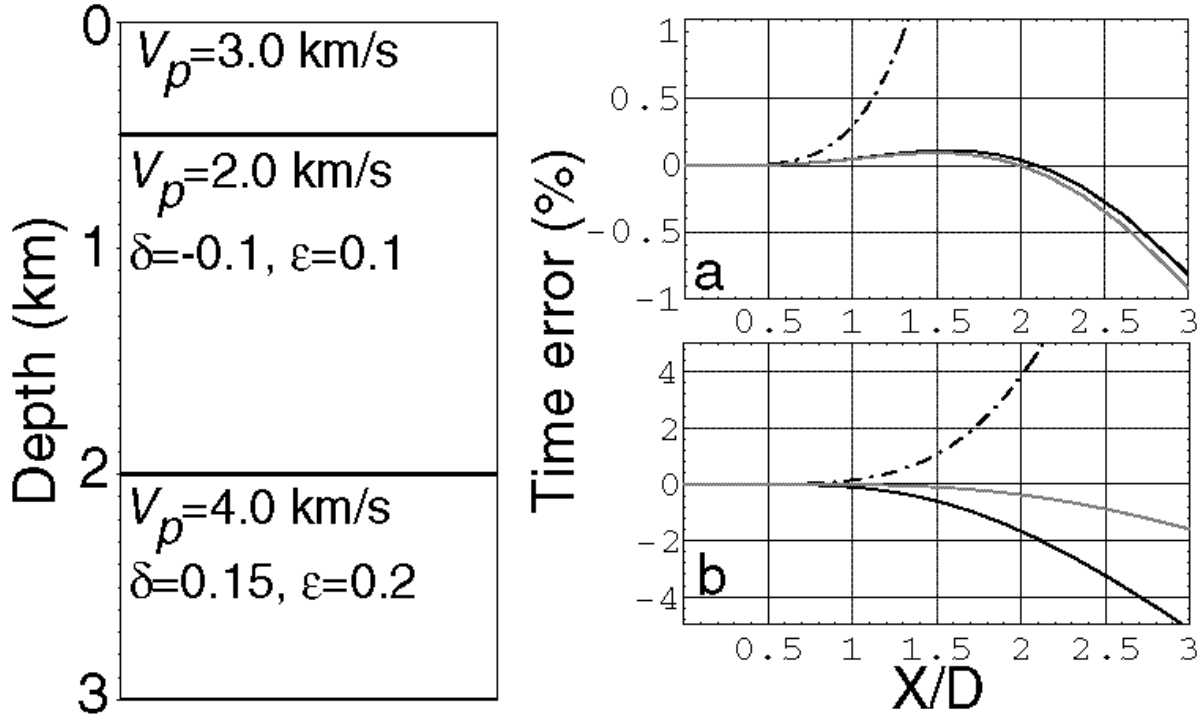

Figure 1. Left: three-layer model with the first layer being isotropic (δ=0 and ϵ=0). Right: Percent time error in moveout (difference from the exact moveout) corresponding to reflections from (a) the bottom of the second layer, and (b) the bottom of the third layer. The gray curve corresponds to using equation (5) based on the definition of V_h in (10); the black curve corresponds to using equation (4), using Tsvankin and Thomsen's definition of V_h; the dashed curve corresponds using equation (3) (a modification of the equation of Hake et al.). Here, $V_{\rm nmo}$, $\eta_{\rm eff}$, and V_h are calculated using equations (7), (8), and (9), respectively.

$\eta_{\rm eff}$ is independent of v_0; therefore any linear velocity function with the same velocity gradient will lead to the same degree of nonhyperbolic moveout, independent of v_0.

Figure 2 shows $\eta_{\rm eff}$ values as a function of vertical time for three values of velocity gradient, a. All three curves show modest values of $\eta_{\rm eff}$ when compared with η for typical homogeneous TI media [e.g., Taylor sandstone, where $\eta = 0.156$ (Thomsen, 1986)]. This result supports the contention that anisotropy typically introduces larger departure from hyperbolic moveout than does velocity layering. From Figure 2, it seems that the nonhyperbolic moveout at later times is large in $v(z)$ media, but as t_0 increases ($t_0 > 2$ s), since the maximum offset usually remains constant, X/D reduces; therefore, the significance of nonhyperbolic moveout becomes smaller (Al-Chalabi, 1974). In other words, although $\eta_{\rm eff}$ increases with t_0 in Figure 2, the decrease in X/D reduces its influence, and therefore nonhyperbolic moveout due to smooth vertical inhomogeneity is small at all times. In contrast, for homogeneous TI media, $\eta_{\rm eff}$ is constant,

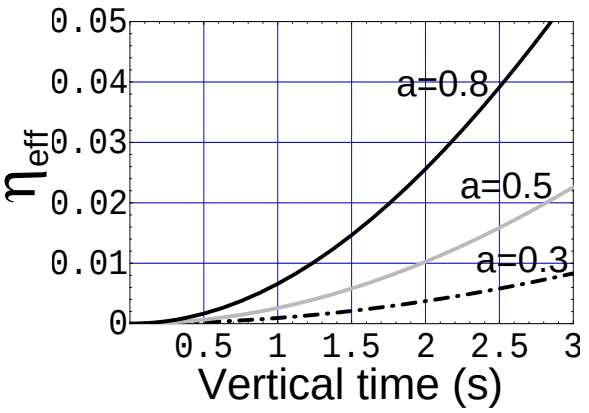

Figure 2. Values of $\eta_{\rm eff}$ in an isotropic medium with constant velocity gradient, as function of zero-offset time t_0, for three values of constant velocity gradient, a.

and the nonhyperbolic moveout is largest at early times where X/D is large.

Following steps similar to those used in deriving equation (11), we can derive an analytical expression of

$\eta_{\rm eff}$ for factorized TI media [i.e., anisotropy parameters η, δ, and ϵ are independent of position (Červený, 1989; Alkhalifah and Larner, 1994)] with linear velocity variation. In factorized TI (FTI) media, we have

$$v_{\rm nmo}(\tau) = v(\tau)\sqrt{1+2\delta}, \tag{12}$$

and

$$v_h(\tau) = v_{\rm nmo}(\tau)\sqrt{1+2\eta_{TI}},$$

where η_{TI} is a constant η value for the factorized TI medium. For such a medium, with constant vertical gradient in the vertical P-wave velocity, $\eta_{\rm eff}$ is given by

$$\eta_{\rm eff} = \frac{1}{8}[(1+8\eta_{TI})\frac{0.5\,a\,t_0}{\tanh(0.5\,a\,t_0)} - 1]. \tag{13}$$

The difference between the $\eta_{\rm eff}$ values for FTI media [equation (13)] and for isotropic media [equation (12)] is given by

$$\Delta\eta_{\rm eff} = \eta_{TI}\frac{0.5\,a\,t_0}{\tanh(0.5\,a\,t_0)}. \tag{14}$$

Based on equation (3), $\Delta\eta_{\rm eff}$ describes the difference in the moveout curves for the two media. Moreover, since the moveout curve described by equation (3) is a reasonable approximation to the zero-offset diffraction curve, even in layered media, the difference between the moveout curves associated with VTI media and those of isotropic media can provide some insight into errors that can result from using an isotropic migration in VTI media.

Estimating Anisotropy Using Nonhyperbolic Moveout

If the maximum offset is large enough (offsets in marine surveys nowadays often exceed 4 km) relative to reflector depth and the resolution of the data is high, it is possible to estimate the degree of nonhyperbolic moveout due to anisotropy.

For $X/D < 1$, in layered VTI media the moveout is approximately hyperbolic and is given by

$$t_h^2 = t_0^2 + \frac{X^2}{V_{\rm nmo}^2}.$$

Subtracting equation (5) from this equation, and replacing η with $\eta_{\rm eff}$, results in

$$\Delta t^2 = t_h^2 - t^2 = \frac{2\eta_{\rm eff}X^4}{V_{\rm nmo}^2[t_0^2V_{\rm nmo}^2 + (1+2\eta_{\rm eff})X^2]}, \tag{15}$$

the amount of time-squared deviation attributable to the nonhyperbolic moveout. A straightforward manipulation of equation (15) results in

$$\eta_{\rm eff} = \frac{\Delta t^2V_{\rm nmo}^2(t_0^2V_{\rm nmo}^2 + X^2)}{2X^2(X^2 - \Delta t^2V_{\rm nmo}^2)}, \tag{16}$$

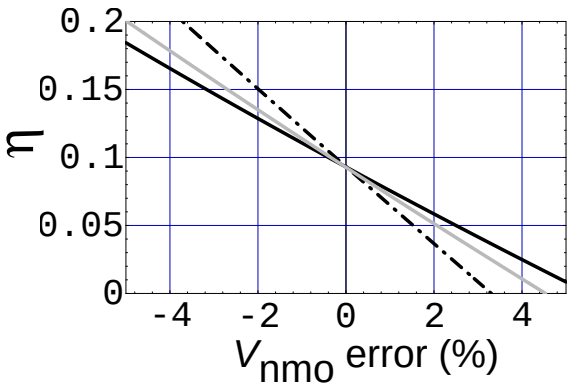

Figure 3. Calculated η values as a function of error in the NMO velocity for offset-to-depth ratios, X/D=1.5 (dashed black curve), X/D=2 (solid gray curve), and X/D=2.5 (solid black curve). Here, t_0=2.0 s, and η for the model is 0.1.

to accuracy governed by that of equation (5). Note that this expression is singular for $X = 0$. Clearly, no $\eta_{\rm eff}$ information can be extracted from small offsets; the stability in estimating $\eta_{\rm eff}$ is expected to increase with offset.

To estimate $\eta_{\rm eff}$ using equation (16), one must first obtain $V_{\rm nmo}$, the short-spread NMO velocity corresponding to a horizontal reflector. This velocity can be obtained using conventional velocity analysis based on a moveout spread that satisfies X/D <1. Assuming that an accurate $V_{\rm nmo}$ is obtained, then Δt^2 can be measured from the reflection moveout in the seismic data. One way to measure Δt^2 for use in equation (16) is to, apply an NMO correction using $V_{\rm nmo}$ and compute

$$\Delta t^2 = t_0^2 - t_{\rm cor}^2, \tag{17}$$

where $t_{\rm cor}$ corresponds to the moveout traveltime after NMO correction. Clearly, if the true moveout is hyperbolic, then $t_{\rm cor}$ equals t_0 and therefore Δt^2=0.

If we assume horizontal layering, the accuracy of the derived $\eta_{\rm eff}$ depends primarily on the accuracy of the measured $V_{\rm nmo}$ and Δt^2, which in turn depends on the accuracy of $V_{\rm nmo}$. Therefore, the sensitivity measure must combine the influences of errors in $V_{\rm nmo}$ on both Δt^2 and $\eta_{\rm eff}$. Figure 3 shows the sensitivity of $\eta_{\rm eff}$ to errors in the measured $V_{\rm nmo}$ (i.e., from velocity analysis), calculated using equation (16). This example corresponds to a homogeneous medium with $\eta = 0.1$, $V_{\rm nmo} = 2.0$ km/s, and $t_0 = 2.0$ s.

As expected, errors are smaller when longer offsets are used in estimating $\eta_{\rm eff}$, again as long as velocity does not vary laterally. Therefore, any inversion technique (i.e., least-squares) based on the nonhyperbolic method to obtain $\eta_{\rm eff}$ from measurements at different offsets should benefit from weighting factors that favor the

far offsets. Further, for fixed offset, the errors clearly increase with increase in either t_0 or $V_{\rm nmo}$ since an increase in either implies a reduced ratio X/D.

Note in Figure 3 that even at zero error in $V_{\rm nmo}$ the inverted $\eta_{\rm eff}$ is not exactly 0.1. The error can be attributed to the difference between the forward time calculation, which involves exact ray tracing, and the inversion process based on equation (16), which is an approximation. This difference in this homogeneous model is largest for about X/D=2.

In any case, the errors caused by equation (16), at the correct $V_{\rm nmo}$, are small for typical anisotropies. Therefore, I rely on this analytical representation to accomplish most of the inversions in this paper.

The above approach of estimating $V_{\rm nmo}$ and η is introduced to develop insights in the nonhyperbolic inversion problem. A more practical approach, based on the 2-D semblance analysis method, is discussed later.

Semblance Analysis Based on Hyperbolic Moveout

Semblance analysis is less sensitive to traveltime errors than is traveltime inversion, and generally produces more stable results. The semblance coefficient is defined as the ratio of the output energy over a window of a stack of traces to the input energy in the unstacked traces. In mathematical terms, S_k, the semblance coefficient, is

$$S_k = \frac{\sum_{l=k-N/2}^{k+N/2}[\sum_{i=1}^{M} f_{ij\,(i,l)}]^2}{M\sum_{l=k-N/2}^{k+N/2}\sum_{i=1}^{M} f^2_{ij\,(i,l)}},$$

where f_{ij} is the recorded data in trace i at the time sample j, and j is a function of the zero-offset time sample l and the trace (offset) i. The window size $N+1$, usually set at about half the dominant period of the wavelet, is used to smooth the semblance-spectrum estimates. The semblance coefficient has a maximum value of unity (when all traces are identical) and a minimum of zero. Semblance summation in this form is biased against randomness and sudden variations in amplitude and polarity. Also, unlike simple summation as in conventional stacking, it is insensitive to the overall trace amplitude. Specifically, events with identical moveout, but differing in amplitude by a scaling factor, produce the same semblance response.

Estimating $V_{\rm nmo}$ through semblance velocity analysis is based on summing data over hyperbolic trajectories controlled by the trial moveout velocity, which defines $j(i,l)$. Therefore, the velocity panel that shows the highest amplitude (stack power), for a specific time, through summation or some semblance measure, is the stacking velocity. In homogeneous isotropic media, where the moveout is hyperbolic, the stacking velocity is identical to the NMO velocity of the medium. In anisotropic, as well as inhomogeneous media (Al-Chalabi, 1974), the moveout is no longer hyperbolic, and the nonhyperbolic portion of the moveout can distort estimates of stacking velocity so that they differ from the NMO velocity, with difference proportional to the size of the nonhyperbolic moveout. As demonstrated earlier, nonhyperbolic moveouts are larger for typical anisotropy than for typical vertical inhomogeneity. Therefore, the difference between the stacking and the NMO velocity is expected to be larger in anisotropic media. For $\eta > 0$, which is the typical situation, moveouts at far offsets deviate from the nearly hyperbolic trajectory at lower times, resulting in higher stacking-velocity estimates from velocity analysis. The size of the deviation of stacking-velocity estimates depends primarily on the range of offsets used in the velocity analysis process.

Figure 4 shows velocity analysis panels for various offset-to-depth ratios (X/D) used in the analysis. Here, the reflection is at t_0=2.0 s, η for the model is 0.1, and $V_{\rm nmo}$=2.0 km/s. Random noise with an rms signal-to-noise ratio of 3 was added to all synthetic examples used in this paper. Estimated stacking velocities increase with increasing X/D; for X/D=2, even the reflection time is distorted from the actual zero-offset time of 2 s. While this spread-length bias increases with increasing X/D, the ability to resolve the velocity also increases with increasing offset used in the analysis process. For X/D=1, which is typically used in conventional velocity analysis, the stacking velocity from Figure 4 is estimated to be 2.03 km/s, 1.5 percent higher than $V_{\rm nmo}$. If a smaller X/D is used (i.e., X/D=0.5), the error in estimating $V_{\rm nmo}$ becomes less than one percent, although the resolution is poorer. Theoretically, as offset approaches zero the stacking velocity should approach $V_{\rm nmo}$. Practically, however, as the range of offsets used decreases, velocity analysis suffers from reduced resolution. The trade off between resolution and accuracy in stacking velocity depends mainly on the peak frequency of the wavelet. Once a choice is made regarding this trade off, we can use Figure 3 to relate possible $V_{\rm nmo}$ errors to the accuracy expected in inverting for η from traveltimes picks.

Figure 5 shows semblance results from summing again over hyperbolic trajectories, controlled by the stacking velocity, for a single reflection event with zero-offset time of 2 s. The general model is the same as in Figure 4 with (a) $\eta = 0$ (isotropic model), and (b) $\eta = 0.1$. In both cases $V_{\rm nmo}$=2.0 km/s. The vertical axis in Figure 5 corresponds to the maximum offset used in the semblance-analysis process. For smaller maximum off-

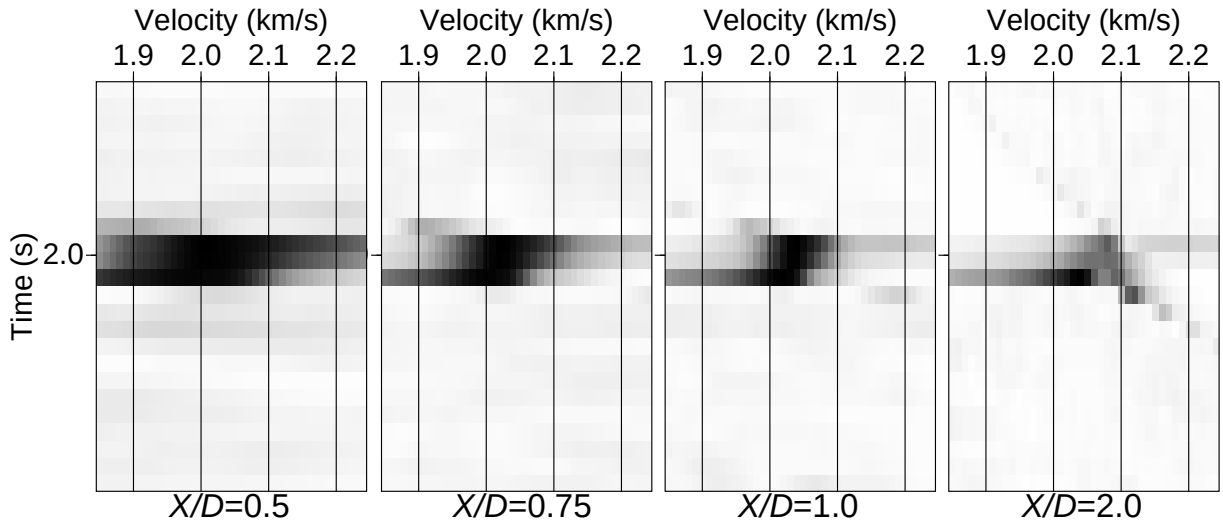

Figure 4. Velocity analysis panels for various offset-to-depth ratios (X/D) used in the analysis. Here, the reflection is at t_0=2.0 s (at depth, D=2 km), η for the model is 0.1, and $V_{\rm nmo}$=2.0 km/s. The peak frequency of the Ricker wavelet used in the analysis here, and throughout the paper, is equal to 40 Hz.

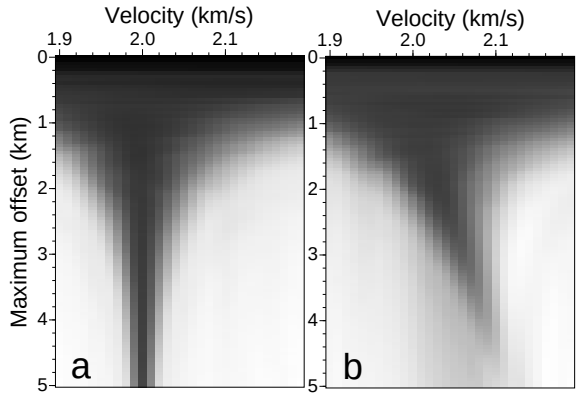

Figure 5. Velocity-analysis panels for various maximum offsets used in the analysis. Here, the reflection is at t_0=2.0 s, $V_{\rm nmo}$=2.0 km/s, and (a) η=0, and (b) η = 0.1. The peak frequency of the Ricker wavelet used the analysis is equal to 40 Hz.

sets, the resolution is poor and the velocity is unresolvable. As the maximum offset increases, so does the resolution. Nevertheless, a clear shift of the best-fit stacking velocity occurs in the TI model, a direct influence of nonhyperbolic moveout. The shift is dramatic as we approach X/D=2 (at offset 4.0 km). Also, as the maximum offset used increases, the semblance power decreases, because the best-fit hyperbolic moveout fails to simulate the true nonhyperbolic moveout. As the amplitude decreases, the contribution of noise to the analysis process would increase. In the next section, I demonstrate, through a semblance analysis over nonhyperbolic moveout, how to reduce the errors in estimating $V_{\rm nmo}$ that arise in long-offset data.

Semblance Analysis Based on Nonhyperbolic Moveout

To use the semblance coefficient with a nonhyperbolic moveout trajectory I simply describe $j(i,l)$ using the nonhyperbolic moveout equation (5) instead of the hyperbolic one. However, in this case, the moveout depends on two parameters rather than one, thus expanding the dimensionality of the search. The nonhyperbolic scan below is applied over V_h and $V_{\rm nmo}$, rather than η and $V_{\rm nmo}$, so that both axes have the same units to simplify comparison of resolution and accuracy.

Figure 6 shows the semblance coefficient as a function of $V_{\rm nmo}$ and V_h for a model with a horizontal reflector at depth 2.0 km beneath a homogeneous TI medium with $V_{\rm nmo}$=2.0 km/s and η=0.2. The zero-offset reflection time of the Ricker wavelet was at 2 s, and the scan was done by setting t_0 = 2.0 s. A 3-D scan would require a search over zero-offset time, as well. Figure 6a corresponds to a maximum X/D of 1.5 used in the semblance summation, Figure 6b corresponds to maximum X/D=2.0, and Figure 6c corresponds to maximum X/D=2.5. As expected, resolving power (reciprocally related to the overall size of the elongated nearly elipsoidal-shaped darkened region) increases with larger maximum

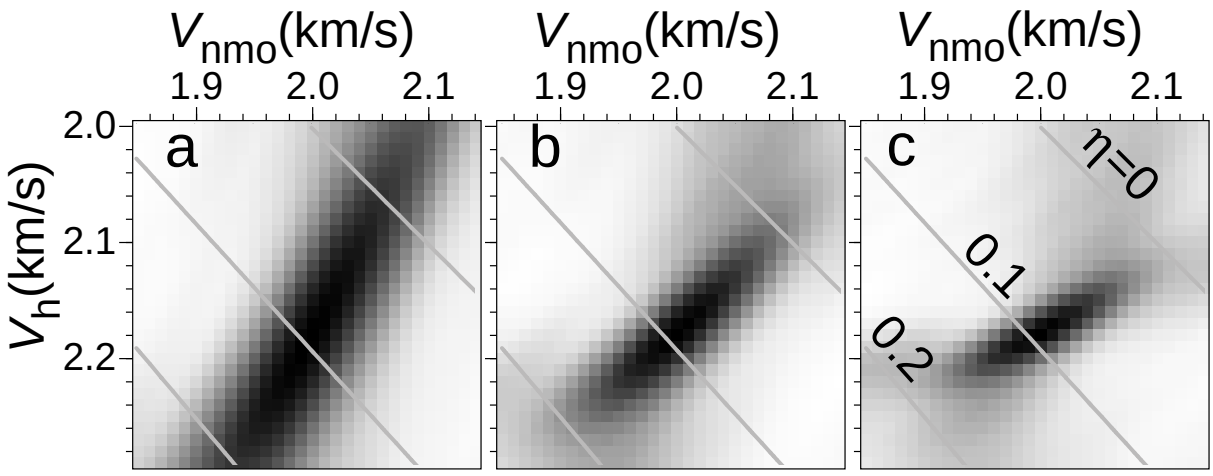

Figure 6. Nonhyperbolic velocity analysis using (a) X/D=1.5 km/s, (b) X/D=2.0 km/s, and (c) X/D=2.5 km/s. Here, the reflection is at t_0=2.0 s, η for the model is 0.1, and $V_{\rm nmo}$=2.0 km/s. The gray curves are contour lines for η based on equation (1). The peak frequency of the Ricker wavelet used in the analysis is 40 Hz.

offsets. In fact, because this elongated region tilts further from the vertical as X/D increases, the ability to resolve V_h increases considerably when larger offsets are included. (The maximum semblance response for any of the three maximum X/D could be picked at $V_{\rm nmo}$=2.0 km/s and V_h=2.18 km/s. (The confidence in this pick increases with increasing offsets used in the analysis.) These values of $V_{\rm nmo}$ and V_h result in $\eta = 0.095$, which is close to the actual value of 0.1. The slightly low estimate for η arises from using the nonhyperbolic equation (5) which is an approximation (although a good one) of the actual moveout.

A practical approach, which can reduce the cost of a 3-D scan over $V_{\rm nmo}$, V_h and t_0 is an iterative 2-D technique, where we scan once over $V_{\rm nmo}$, fix the interpreted values of $V_{\rm nmo}$, and then do another scan, this time over V_h. The results of the V_h analysis would then be used to scan again over $V_{\rm nmo}$ and so on until a convergence criterion is met. As has been suggested by May and Stratley (1979), convergence is guaranteed through using an orthonormal basis (i.e. the Legendre polynomials) to represent the moveout polynomial [equation (3)].

The NMO velocity obtained from semblance analysis is usually more accurate than that extracted by fitting a hyperbolic curve, in a least square sense, to the moveout of a reflection. We should expect a similar result when nonhyperbolic moveouts are used in the semblance. In the analysis based on least-squares fitting of traveltimes, Tsvankin and Thomsen (1995) concluded that the second and fourth order coefficients of the Taylor's series expansion of the TI moveout are not resolvable from traveltime moveout curves in VTI media. The reason that the semblance approach reduces this ambiguity in resolving the anisotropy parameters discussed by Tsvankin and Thomsen is basically described by the concept of objective function (a function of the unknown parameters formed so that maximum or minimum value of the function corresponds to the solution of the problem).

The objective function for the semblance analysis approach, given by the semblance responses in Figure 6 for 40-Hz peak frequency, has a more stable maximum than does the objective function calculated based on a least-square traveltime fitting of the moveout over the same range of offsets (Figure 7). In fact the least-square method is more sensitive to the shortcomings of the moveout approximation than is the semblance approach. This is obvious by observing the amount of shift of the maximum (or minimum) from the true values for the model. The velocity-analysis objective function is also more stable and less sensitive to noise and traveltime errors than is the least-squares traveltime fitting approach. Figure 8 shows (a) a semblance analysis, and (b) a least-squares traveltime fitting objective function after subjecting the synthetic data of Figure 6 to random traveltime shifts between 0 and 0.5%(=10 ms), as might happen after a poor static correction. These traveltime shifts have a mean of 0.25%(=5 ms). Clearly, the objective function of the least-square fitting approach is much more influenced by the errors (shifted from the true value) than is the semblance approach. The resolution of the objective function for the semblance approach also depends largely on the peak frequency of the wavelet. The dominant frequency of 40 Hz, used here, is quite representative of

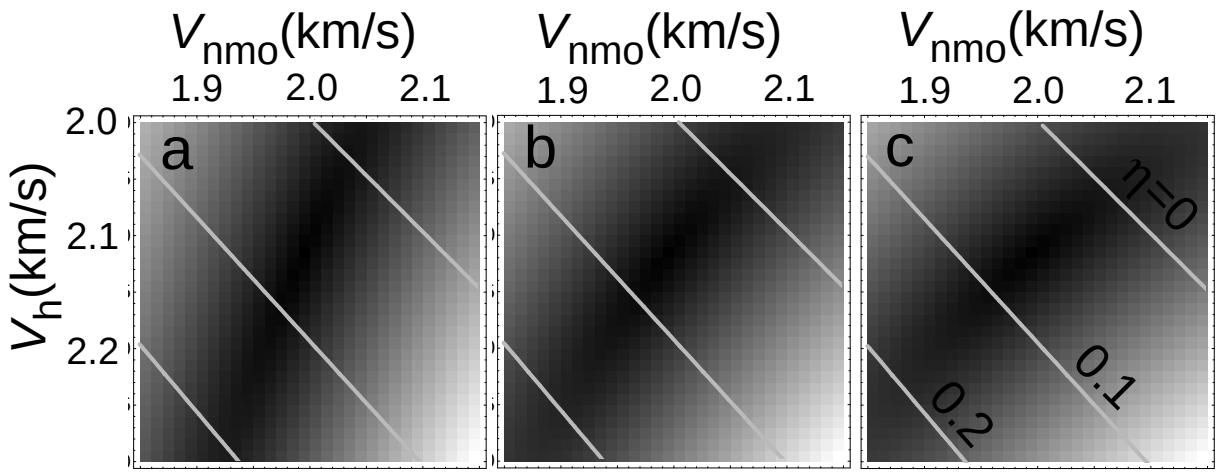

Figure 7. Root-mean-square sum of the difference between the actual moveout and the moveout given by equation (4) as a function of V_h and $V_{\rm nmo}$ using (a) X/D=1.5 km/s, (b) X/D=2.0 km/s, and (c) X/D=2.5 km/s. This is the same model as in Figure (6), where the reflection is at t_0=2.0 s, η for the model is 0.1, and $V_{\rm nmo}$=2.0 km/s.

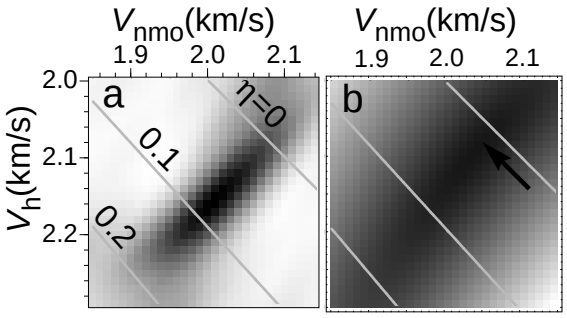

Figure 8. Objective functions for (a) semblance analysis and (b) for least-square fitting, for an X/D=2, same as Figures (6)b and (7)b, respectively, after adding random traveltime shifts between 0 and 0.5% (=10 ms) to the data. The arrow in (b) points to the peak which is severely shifted due to the added errors.

frequencies in seismic data. More error-analysis studies can be found in Grechka and Tsvankin (1996).

Anisotropy and Inhomogeneity

In typical TI media, η is positive, and the fourth-order term in equation (5) is negative. Similarly, in typical isotropic media in which velocity varies with depth, the fourth-order term is again negative, producing a similar moveout behavior. Specifically, both $t^2 - X^2$ curves are convex upwards (Hake et al., 1984). Although $\eta_{\rm eff}$ for isotropic media is usually smaller than that in TI media, such a result will raise problems in deciding how much of the inverted $\eta_{\rm eff}$ to attributr to anisotropy and how much to inhomogeneity. Nevertheless, we expect that, often, the dominant portion of the nonhyperbolic moveout can be attributed to anisotropy, and if inhomogeneity is resolvable through other techniques (i.e., conventional velocity analysis), then a better assessment of the contribution from anisotropy can be obtained.

The relative sensitivity of dip-moveout processing to anisotropy and vertical inhomogeneity differs from that of nonhyperbolic moveout. For example, primarily for moderate to low dips, a dip-moveout impulse response for typical anisotropy ($\eta > 0$) can be approximated as a stretched version of the one for homogeneous isotropic media, while the $v(z)$ isotropic impulse response is a squeezed version of the homogeneous isotropic one (Alkhalifah, 1996a). Therefore, the presence of both anisotropy and inhomogeneity in a medium leads to DMO actions that are opposite to one another, while the actions of both anisotropy and inhomogeneity increase the nonhyperbolic moveout of reflections from horizontal interfaces.

Suppose only one reflection is strong enough to show measurable nonhyperbolic moveout in a $v(z)$ VTI medium. A reasonable approach might be to consider the medium FTI, and therefore obtain a constant η_{TI}. Using equation (8) and setting $\eta(\tau)$ to be constant ($=\eta_{TI}$) results in

$$\eta_{TI} = \frac{1}{8}[(1+8\eta_{\rm eff})\frac{V^4_{\rm nmo}(t_0)}{\frac{1}{t_0}\int_0^{t_0} v^4_{\rm nmo}(\tau)d\tau} - 1], \qquad (18)$$

which enables one to deduce an average η corresponding solely to anisotropy. Equation (18) is important because often, as we will see later in the field example especially

at early recording times ($t_0 < 2$ s), only one reflection will be strong enough to show measurable nonhyperbolic moveout. (Lateral velocity variation, of coarse, would complicate this interpretation.)

Advantages of the Nonhyperbolic Inversion Method

Alkhalifah and Tsvankin (1995) have developed a procedure for estimating η and $V_{\rm nmo}$ in layered TI media using the short-spread moveout behavior for dipping reflectors (DMO method). Even vertical variations of η can be estimated using such a DMO method (Alkhalifah, 1996b). That DMO-based procedure is probably more stable in inverting for the anisotropy parameters than is the method described above, especially in the absence of large offsets and at later times, where X/D is small.

Unlike the DMO method, however, this nonhyperbolic moveout method does not require dipping reflectors, and therefore, it is more flexible; also, it can be applied to a broader range of field data. Moreover, it is easier to use to obtain lateral variations of η. For example, statistical estimation of the lateral variation in η can be made from data at many CMP locations.

Given the tradeoff between $V_{\rm nmo}$ and η in equation (1), the errors in estimating V_h, using the nonhyperbolic moveout, are generally small. The horizontal velocity is the necessary quantity for migration of a vertical reflector to its true position, and using the nonhyperbolic inversion it is usually estimated at higher accuracy than is $V_{\rm nmo}$. Therefore, with the nonhyperbolic moveout method one can better construct the time-migration impulse response than with isotropic methods.

One area in which η measurements from nonhyperbolic moveout can play a major role is in the presence of very steep (near vertical) reflectors, such as flanks of salt domes in the Gulf of Mexico, where, in addition, reflections from interfaces with intermediate dips may not be available. Alkhalifah and Tsvankin (1995) showed that the DMO method fails to yield accurate values of η for such steep dips, primarily because the moveout for such reflections in TI media is not distinguishable from that in isotropic media or in any other anisotropic model. Therefore, the moveout for such dips becomes somewhat independent of the anisotropy parameter, η. The nonhyperbolic moveout for events from sub-horizontal reflectors potentially can provide η information for improved migration of data from steep reflectors.

This nonhyperbolic method, however, is based on the assumption of lateral homogeneity, with some tolerance, as is usually the case with $v(z)$ algorithms, to mild lateral inhomogeneity (i.e., smooth lateral variations). Therefore, strong lateral inhomogeneities will cause problems for the method, requiring a much more advanced treatment, which is beyond the scope of this paper. In media with strong lateral inhomogeneity, $\eta_{\rm eff}$ is still possibly measurable, and can be used to aid in making nonhyperbolic moveout correction, but it has no simple interpretation in terms the medium properties.

Field-Data Example

Figure 9 shows a seismic line from offshore Africa provided by Chevron Overseas Petroleum, Inc. The line was processed using conventional NMO and DMO algorithms without taking anisotropy into account. Velocity analysis shows a general vertical velocity increase with depth that can be simplistically modeled with a constant gradient of about 0.7 s^{-1}. As Alkhalifah and Tsvankin (1995) demonstrate, these data are influenced by the presence of anisotropy. Moreover, using the DMO method for estimating η and $V_{\rm nmo}$, Alkhalifah (1996a) shows that the anisotropy is strongest above t_0=2 s, in a massive shale formation.

Figure 10 shows CMP gathers after applying isotropic homogeneous DMO and NMO correction. The NMO correction is based on the velocities obtained from conventional velocity analysis, using a spread given by $\frac{X}{D} < 1$. DMO was applied to reduce even the small distortion of the stacking velocity caused by the mild dip ($\simeq$6 degrees) of the reflector at about t_0=1.8 s. The two subparallel events prior to t_0=2.0 s show significant departure from hyperbolic moveout. If the deviations in Figure 10 were caused by NMO velocity overcorrection (using lower than true velocities), then these moveout curves would have departures from t_0 proportional to X^2. The fact that these curves are practically straight for $\frac{X}{D}$ <1, implies that they are controlled by higher-order terms of the Taylor's expansion (e.g., X^4).

A detailed portion of Figure 10 (Figure 11) helps in picking reflection times, and therefore, measuring Δt^2. Some of the moveouts (e.g., the reflection at t_0=1.86 s at CMP 700) have a slight initial plunge prior to the larger offsets where the nonhyperbolic behavior dominates the moveout. This initial plunge results from using a $V_{\rm nmo}$ value in the NMO correction that is higher than the true value. As suggested in Figure 4, the higher velocity is probably due to spreadlength bias, which arises from the attempt to fit nonhyperbolic moveout with hyperbolic curves. Analysis over nonhyperbolic moveout should overcome such a problem as well as provide an estimate of the nonhyperbolic portion of the spread.

Figure 12 shows the semblance response using nonhyperbolic moveouts as a function of $V_{\rm nmo}$ and V_h (sim-

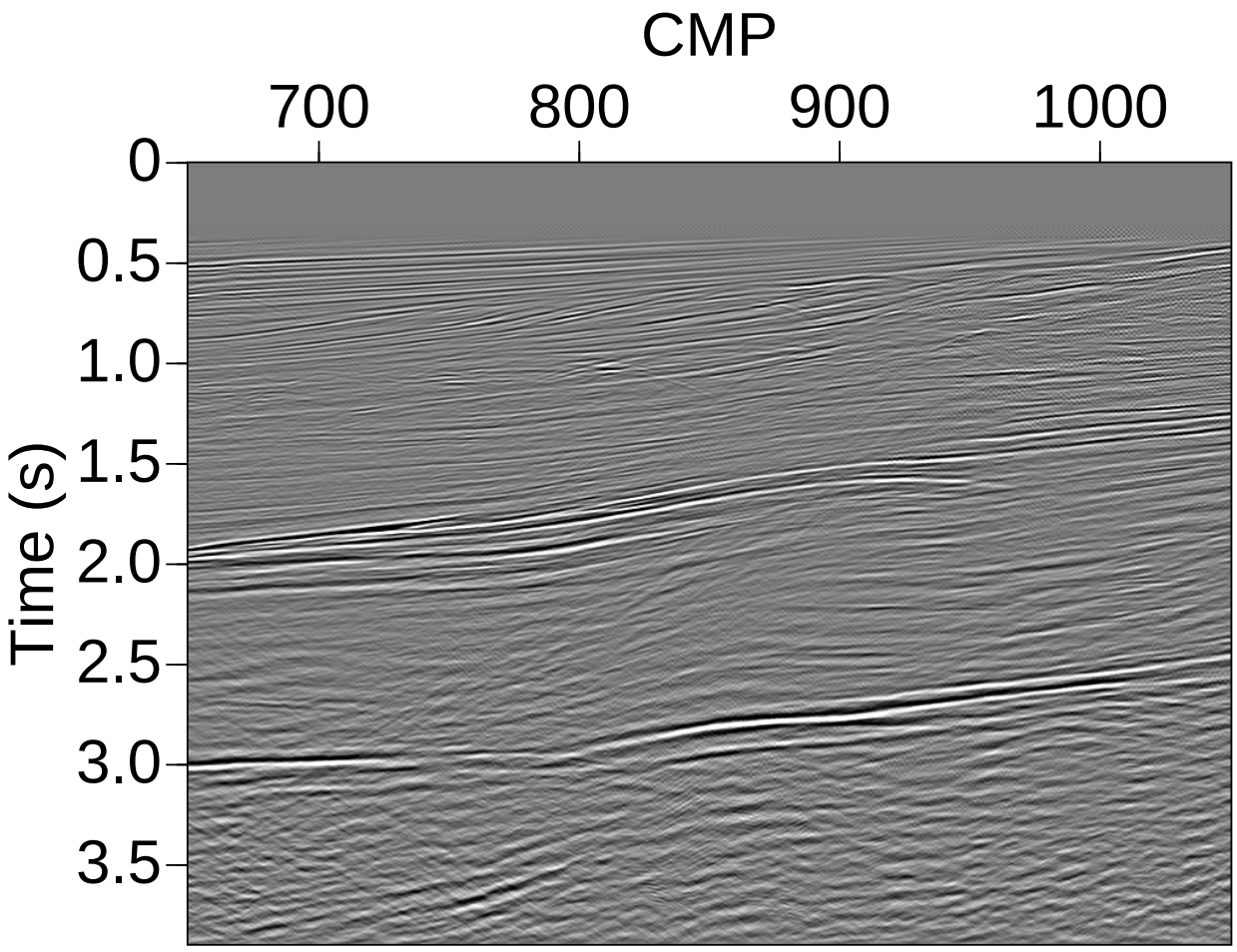

Figure 9. CMP-stacked seismic line (offshore Africa) after application of NMO correction along with homogeneous and isotropic DMO; the distance between CMP's is 12.5 m.

ilar to that of Figure 6), for the same reflection events shown in Figure 11, at CMP locations 700, 800, and 900. Note that, among the three locations, $V_{\rm nmo}$ decreases monotonically from 2.15 km/s at CMP location 700 to 2.07 km/s at CMP 900. This decrease corresponds mainly to the decrease in the zero-offset times of these reflections, which reflects the general velocity increase with depth obtained by Alkhalifah (1996a). On the other hand, V_h or η have their highest value at the middle location, CMP location 800. At this CMP location $\eta_{\rm eff}$=0.28, whereas at CMP locations 700 and 900 $\eta_{\rm eff}$ equals 0.2 and 0.16, respectively. These values of η include the combined influence of anisotropy and inhomogeneity. Using equation (18) in an attempt to remove the influence of vertical inhomogeneity, I estimate η_{TI}=0.15, 0.22, and 0.13 for CMP locations 700, 800, and 900, respectively, which I attribute primarily to the anisotropy. These values are on average higher than those obtained by Alkhalifah and Tsvankin (1995) and Alkhalifah (1996a with the DMO-based approach. However, their measurements correspond primarily to the region near CMP location 900, which has an η value that is more in agreement with their calculations. Finally, considering the overall small lateral velocity variation, the resulting estimate of η suggests the presence of anisotropy. Further analysis of the relative importance of anisotropy and lateral velocity variation, however, is necessary.

Figure 13 shows a schematic plot of the raypath from the source down to the reflection point and back up to the receiver, for the maximum offset used in the semblance analysis at CMP 800 in Figure 12. The ray bending is caused by the vertical increase in velocity with depth. Unlike NMO velocity analysis, the η estimates rely on information from large offsets; therefore, the subsurface influence on the η estimate is not laterally local (i.e., near the CMP location of measurement). Although use of large

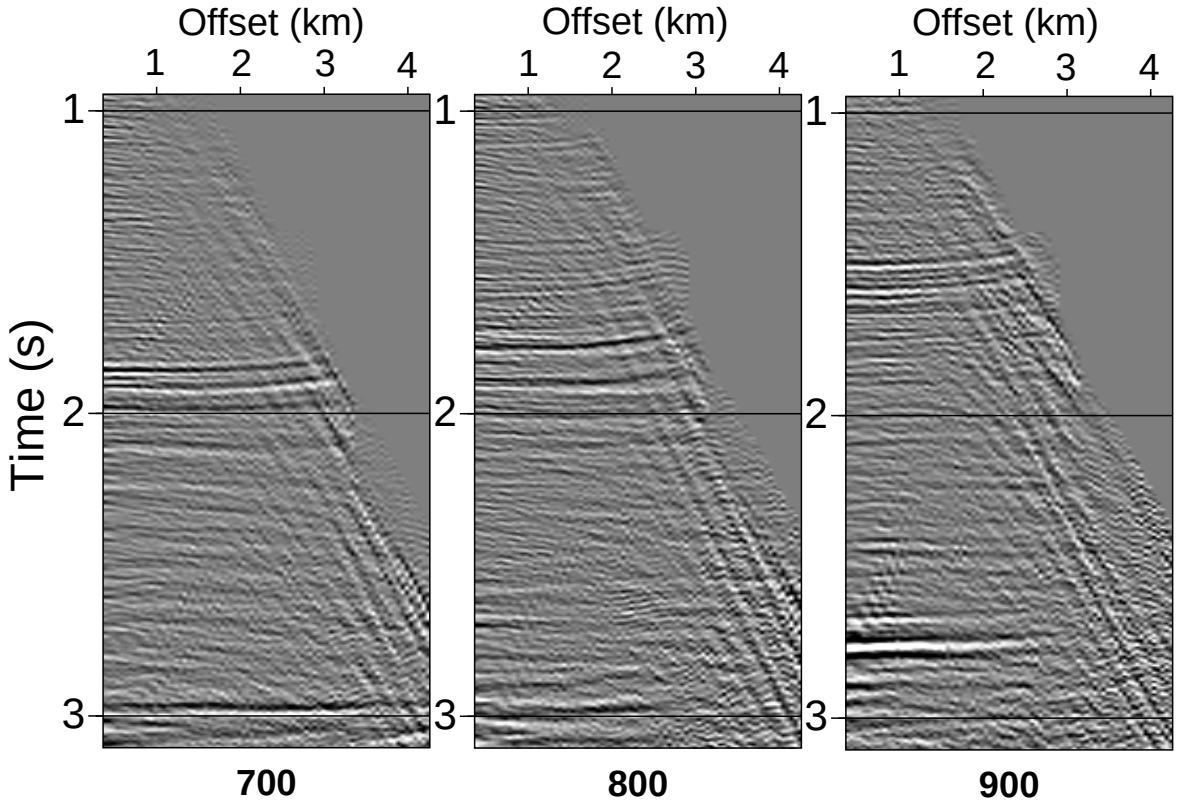

Figure 10. CMP gathers at locations 700, 800, and 900 after NMO correction and isotropic homogeneous DMO. The NMO correction is based on velocities obtained from conventional velocity analysis with X/D <1.

offsets can help improve the resolution of the inversion, it can hamper the lateral resolution of estimating η.

To get a better understanding of the lateral variations in η in the above field example, we should compare CMP locations that are at least 3 km apart (the distance corresponding to the maximum offset used in the analysis). Moreover, the data would have better served us if η estimates were made at many more CMP locations and were then averaged (smoothed) over 3 km intervals, with for example a Gaussian window.

Figure 14 shows another portion of the data set from offshore Africa that is dominated by horizontal (or subhorizontal) events. The large number of strong horizontal reflectors should provide us with an excellent setting for applying the layer stripping approach discussed earlier. This data set also includes offsets up to 4.3 km, which will help in boosting the resolution of the semblance analysis at later times. Nevertheless, the measurements at the later times still suffer from lower resolution, due to smaller X/D, as well as increased layer-stripping errors that propagate from the top to the bottom of the section. Figure 15 shows four sample nonhyperbolic semblance responses calculated at times 1.24, 1.86, 2.28, and 2.99 s, at CMP location 300. Picking the $V_{\rm nmo}$ and V_h values corresponding to the maximum semblance responses for these times, as well as other ones, and inserting them into equations (7) and (8), yields the velocity and η curves shown in Figure 16 (black curves). Because these are marine data, $V_{\rm nmo}$ and η are set to equal 1.5 km/s and zero, respectively, at the surface. The gray curves, on the other hand, describe the upper and lower limits of possible parameter values corresponding to the uncertainties in picking $V_{\rm nmo}$ and V_h (e.g., picking within the dark region in Figure 15). As above, I ignore the influence of lateral velocity variation on the results. However, the lateral velocity variation in this region is mild ($< 2\%$).

Note in Figure 15 that the semblance resolution, especially for V_h, decreases with increasing zero-offset time due to the reduction in X/D. This will degrade the accuracy of picking, resulting in errors in the interval values that increase with vertical time. Also, as with any other layer-stripping application, the interval values at the later times have errors accumulated from measurements at the earlier times. So, in Figure 16, η values beyond t_0=2.0

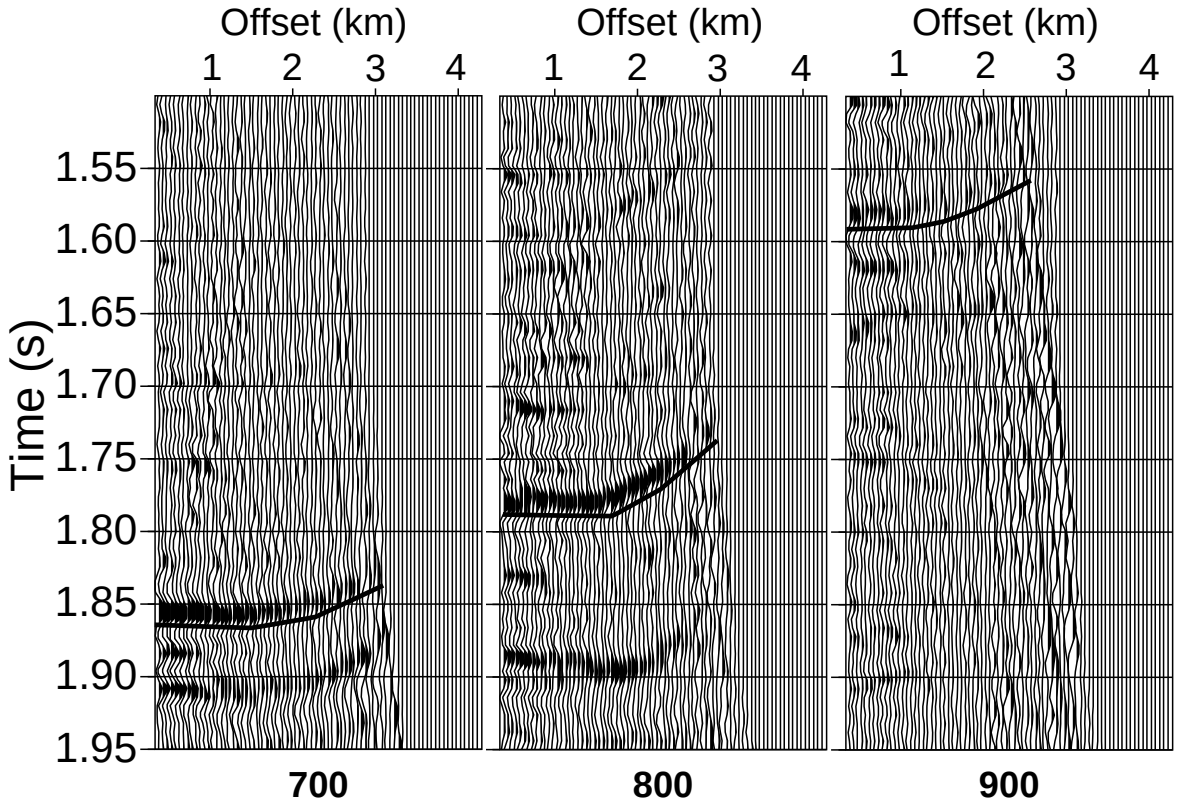

Figure 11. Detail of Figure 10. The black curve is the approximate location of the zero-crossing of the reflection wavelet. It indicates the general shape of the reflection moveout.

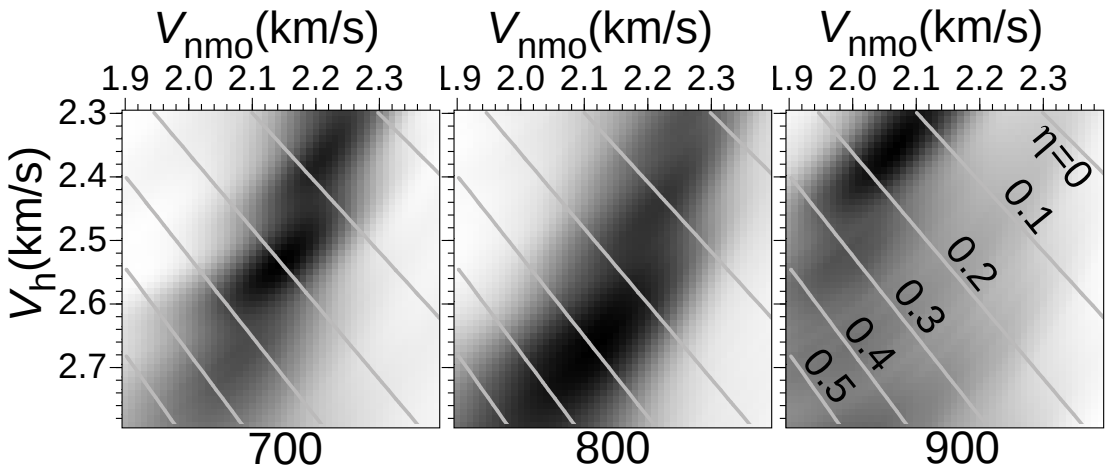

Figure 12. Nonhyperbolic velocity analysis for CMP locations 700, 800, and 900. Here, t_0, which varies from one CMP to another, has been extracted from Figure 11. The gray curves again correspond to contour lines describing η.

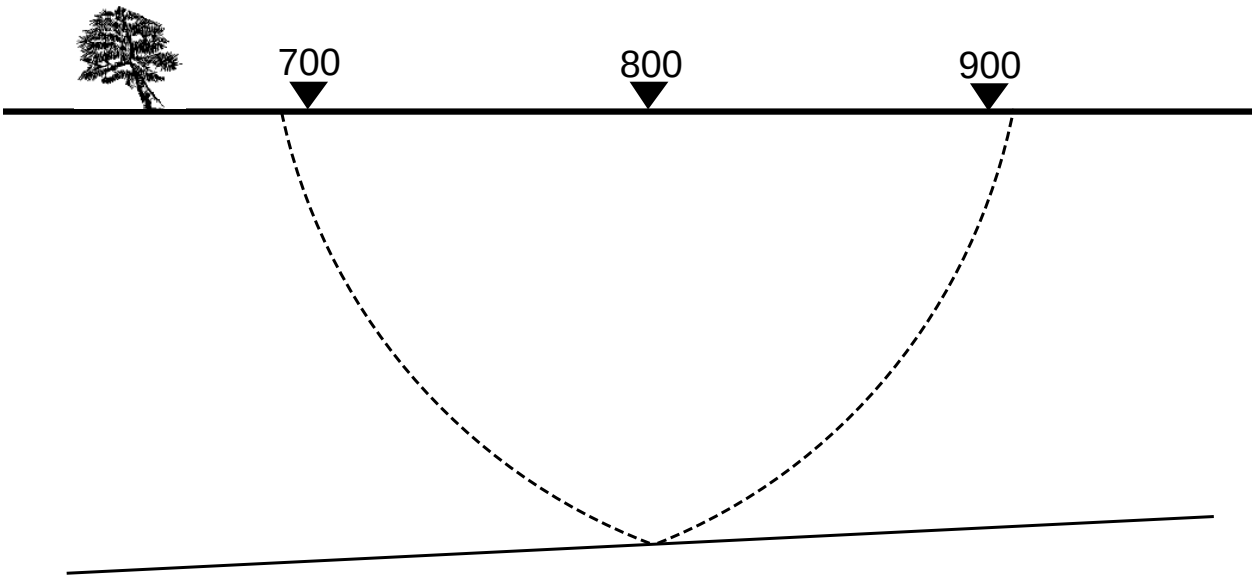

Figure 13. Schematic plot of the raypath for the CMP location at 800 for a ray traveling from the source down to the reflection point and back up to the receiver, based on the maximum-offset raypath used in the analysis.

s are not that reliable. On the other hand, the increase of η up to t_0=1.8 s is believable, because this increase is maintained even when the measured values at $t_0 = 1.86$ s in Figure 15 are perturbed within the range of acceptable picks (the black region). For example, although V_h was evaluated at the maximum semblance to equal 2.05 km/s, one can assume a margin of error, corresponding to the black region, of about $\pm$0.04 km/s, which corresponds to about a 2 percent error. The limits of this margin are given by the gray curves in Figure 16. Within this margin of error, the η curve in Figure 16 always increases up to the maximum value at 1.8 s, but the particular form of the increase depends on the V_h value. Therefore, the increase in η until 1.8 s is more-less an accurate representation of the anisotropy variation under CMP 300. The reliability of the results at these times was further enhanced by observing similar measurements from neighboring CMP locations (i.e., CMP locations 200 and 250).

Conclusions

The nonhyperbolic moveout behavior of reflections from horizontal interfaces is an important source of velocity information for processing, especially in anisotropic media. In most anisotropic media, the nonhyperbolic moveout is relatively large, larger, in fact, than that in typical vertically inhomogeneous isotropic media. Therefore, it is usually observable and measurable, and thus, can be used to invert for medium parameters. Although estimates of η derived from nonhyperbolic moveout method alone might not be reliable to use directly in lithology interpretation, such results can play a major role in processing and supporting the estimates of η and $V_{\rm nmo}$ obtained from the DMO method (Alkhalifah and Tsvankin, 1995), as well as in providing η values in areas where the dipping features required by the DMO method are absent.

The effective η values obtained from the NMO method can be used as an indicator of the relative contribution to nonhyperbolic moveout due to anisotropy as opposed to that due to vertical heterogeneity. This indicator demonstrates that nonhyperbolic moveout associated with typical TI media ($\eta \simeq 0.1$) is greater than that associated with typical $v(z)$ isotropic media; therefore, the importance of applying the nonhyperbolic moveout correction in such TI media prior to stacking is larger than that in $v(z)$ media. The importance of anisotropy relative to that of lateral velocity variation remains an important area for future study.

The process of extracting η values from the nonhyperbolic moveout behavior of reflections is sensitive to errors in the measured $V_{\rm nmo}$, with the sensitivity reducing as offsets used in the inversion increase. It also reduces at smaller vertical time corresponding to smaller depths, and thus larger offset-to-depth ratio. In TI media, with positive η, nonhyperbolic moveout tends to give an overestimate of the value of $V_{\rm nmo}$ obtained us-

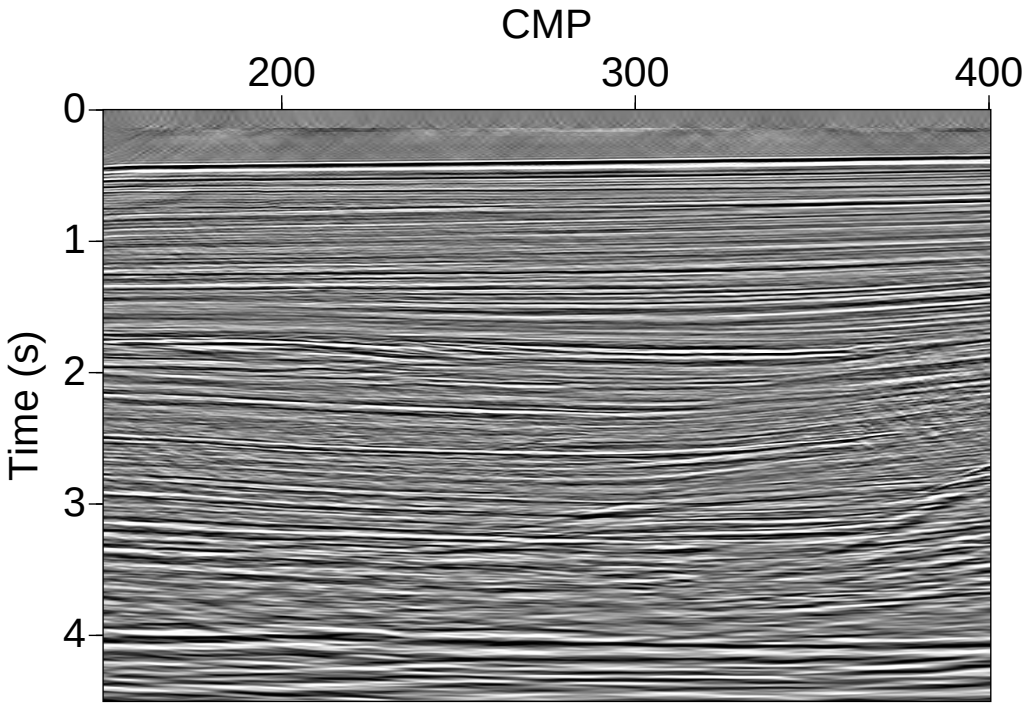

Figure 14. Time-migrated seismic line (offshore Africa). This line is nearby the line shown in Figure 9, but in deeper waters.

ing velocity analysis, depending mainly on the the offset-to-depth ratio, X/D, used in the velocity analysis. For typical $X/D < 1.0$, such increases do not exceed 2 percent. Depending on the ratio X/D used in the inversion for η, this overestimate of $V_{\rm nmo}$ results in an estimate of η that is low, by no more than 0.04 for a model with η=0.1. However, the estimates η and $V_{\rm nmo}$ can be used iteratively to improve further estimates of one another. At increased cost, semblance analysis over nonhyperbolic trajectories can reduce such errors and thereby providing better estimates of $V_{\rm nmo}$ and η.

The nature of seismic data, which are dominated by horizontal and sub-horizontal reflections, makes this method more widely applicable than is the DMO method of Alkhalifah and Tsvankin (1995), which relies on the presence of reflections with different dips. The nonhyperbolic moveout method, in homogeneous media, needs only one reflector, preferably a horizontal one, for the inversion to work. Therefore, it can be applied almost anywhere, which helps in estimating lateral variations in η. Use of larger offsets in the nonhyperbolic inversion, however, which are necessary to stabilize the inversion, can degrade the lateral resolution of η.

One area in which η measurements from nonhyperbolic moveout can play a major role is in the presence of very steep (near vertical) reflectors, such as flanks of salt domes in the Gulf of Mexico, where in addition, reflectors from interfaces with intermediate dip may not be available. In this situation, the DMO method of Alkhalifah and Tsvankin (1995) fails for such steep dips, primarily because the moveout for such a reflection in TI media is not distinguishable from that in isotropic media. Therefore, nonhyperbolic moveout from horizontal events maybe the only information in surface seismic data that can provide us with η estimates necessary to better migrate such dips.

Using the nonhyperbolic moveout method on data from offshore Africa helped to estimate η both vertically and laterally. However, the accuracy of the inversion reduces dramatically with depth, due to the reduced X/D, and due to layer-stripping errors.

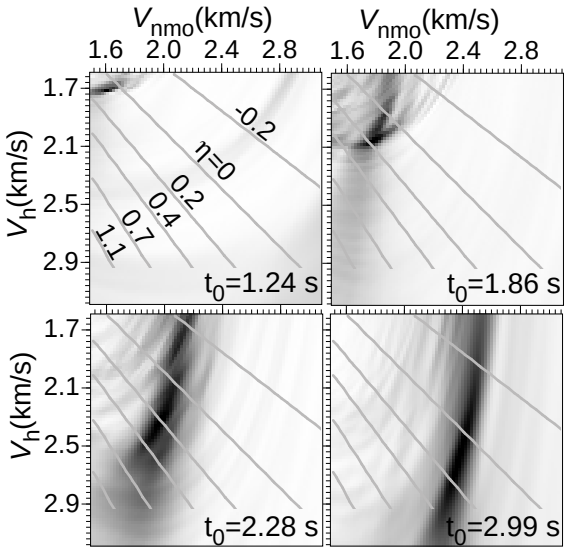

Figure 15. Nonhyperbolic velocity analysis at CMP location 300 in Figure 14 for different t_0 values. The gray curves correspond to contour lines in η_{eff}.

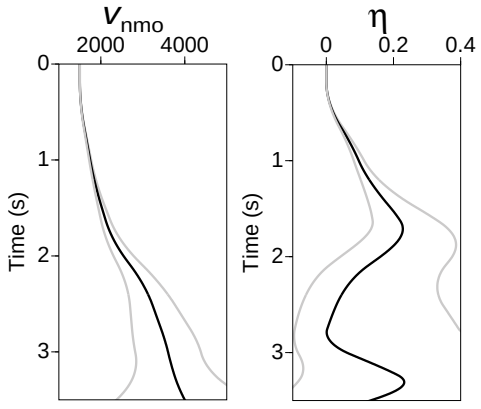

Figure 16. Interval values v_{nmo} and η as a function of vertical time (black curves) at CMP location 300, with the margin of possible values, due to picking uncertainties, laying between the two gray curves.

Acknowledgment

I am grateful to Ken Larner, Ilya Tsvankin, John Toldi and Vladimir Grechka for helpful discussions. I thank John Toldi and Chris Dale of Chevron Overseas Petroleum, Inc. for providing the field data. Special, thanks are also due to the Center for Wave Phenomena, Colorado School of Mines, for its technical support, and also to KACST, Saudi Arabia, for its financial support. Financial support for this work also was provided in part by the United States Department of Energy, (this support does not constitute an endorsement by DOE of the views expressed in this paper).

REFERENCES

Al-Chalabi, M., 1974, An analysis of stacking, rms, average, and interval velocities of horizontally layered ground: Geophys. Prosp., **22**, 458-475.

Alkhalifah, T., 1996a, Transformation to zero offset in transversely isotropic media: Geophysics, expected to be published in the July-August issue.

Alkhalifah, T., 1996b, Anisotropy processing in vertically inhomogeneous media: Geophysics, in print.

Alkhalifah, T., 1996c, Analytic insights into the anisotropy parameter η: Center for Wave Phenomena, Colorado School of Mines (CWP-202).

Alkhalifah, T., and Larner, K., 1994, Migration errors in transversely isotropic media: Geophysics, **59**, 1405-1418.

Alkhalifah, T., and Tsvankin, I., 1995, Velocity analysis for transversely isotropic media: Geophysics, **60**, 1550-1566.

Banik, N. C., 1984, Velocity anisotropy of shales and depth estimation in the North Sea basin: Geophysics, **49**, 1411–1419.

Červený, V., 1989, Ray tracing in factorized anisotropic inhomogeneous media: Geophys. J. Internat., **94**, 575–580.

Dix, C. H., 1955, Seismic velocities from surface measurements: Geophysics, **20**, 68-86.

Gonzalez, A., Levin., F. K., Chambers, R. E., and Mobley, E., 1992, Method of correcting 3-D DMO for the effects of wave propagation in an inhomogeneous earth, 62nd Ann. Internat. Mtg., Soc. Expl. Geophys., Expanded Abstracts, 966–969.

Grechka, V., and Tsvankin, I., 1996, Feasibility of nonhyperbolic moveout inversion in transversely isotropic media: Center for Wave Phenomena, Colorado School of Mines (CWP-203).

Hake, H., Helbig, K., and Mesdag, C. S., 1984, Three-term Taylor series for $t_2 - x^2$ curves over layered transversely isotropic ground: Geophys. Prosp., **32**, 828-850.

Larner, K., 1993, Dip-moveout error in transversely isotropic media with linear velocity variation in depth: Geophysics, **58**, 1442-1453.

Larner, K. and Cohen, J., 1993, Migration error in factorized transversely isotropic media with linear velocity variation with depth: Geophysics, **58**, 1454–1467.

Levin, F., 1990, Reflection from a dipping plane—Transversely isotropic solid: Geophysics, **55**, 851–855.

Malovichko, A. A., 1978, A new representation of the traveltime curve of reflected wave in horizontally layered media: Applied Geophysics, **91**, 47-53.

May, B. T., and Stratley, D. K., 1979, Higher-order moveout spectra: Geophysics, **44**, 1193–1207.

Neidell, N. S., and Taner, M. T., 1971, Semblance and other coherency measures for multichannel data: Geophysics, **36**, 482–497.

Shah, P. M., and Levin, F. K., 1973, Gross properties of time-distance curves: Geophysics, **28**, 643-656.

Taner, M. T., and Koehler, F., 1969, Velocity spectradigital computer derivation and applications of velocity functions: Geophysics, **34**, 859-881.

Thomsen, L., 1986, Weak elastic anisotropy: Geophysics, **51**, 1954–1966.

Tsvankin, I., 1995, *P*-wave signatures and notation for transversely isotropic media: An overview: Geophysics, **61**, 467-483.

Tsvankin, I., and Thomsen, L., 1994, Nonhyperbolic reflection moveout in anisotropic media: Geophysics, **59**, 1290-1304.

Tsvankin, I., and Thomsen, L., 1995, Inversion of reflection traveltimes for transverse isotropy: Geophysics, **60**, 1095-1107.

APPENDIX A: Effective η in Layered Media

For multi-layered TI media, the exact quartic coefficient A_4 of the Taylor's series expansion is given by (Hake et al., 1984; Tsvankin and Thomsen, 1994)

$$A_4 = \frac{\left(\Sigma_i\ [v_{\rm nmo}^{(i)}]^2\Delta t^{(i)}\right)^2 - t_0\ \Sigma_i[v_{\rm nmo}^{(i)}]^4\Delta t^{(i)}}{4\left(\Sigma_i[v_{\rm nmo}^{(i)}]^2\Delta t^{(i)}\right)^4} + \frac{t_0\Sigma_i A_{4i}[v_{\rm nmo}^{(i)}]^8[\Delta t^{(i)}]^3}{\left(\Sigma_i[v_{\rm nmo}^{(i)}]^2\Delta t^{(i)}\right)^4}, \quad \text{(A1)}$$

which includes (in the first term) ray-bending due to the layered structure. Here, $\Delta t^{(i)}$ and $v_{\rm nmo}^{(i)}$ are the two-way zero-offset time and the NMO velocity for a given layer i, respectively. A_{4i} is the quartic coefficient A_4 in layer i. When the contribution of the vertical shear-wave velocity is ignored, it is given by

$$A_{4i} = -\frac{2\eta^{(i)}}{[\Delta t^{(i)}]^2[v_{\rm nmo}^{(i)}]^4}, \quad \text{(A2)}$$

where $\eta^{(i)}$ is the η value for a given layer i. On the other hand, again ignoring the contribution of the vertical shear-wave velocity, A_4 is given by

$$A_4 = -\frac{2\tilde{\eta}_{\rm eff}}{t_0^2 V_{\rm nmo}^4}. \quad \text{(A3)}$$

Plugging A_{4i} into equation (A1) and using integration instead of summation gives

$$A_4(t_0) = \frac{t_0^2 V_{\rm nmo}^4(t_0) - t_0\ \int_0^{t_0} v_{\rm nmo}^4(\tau)d\tau}{4t_0^4 V_{nmo}^8} - \frac{8t_0\int_0^{t_0}\eta(\tau)v_{\rm nmo}^4(\tau)d\tau}{4t_0^4 V_{nmo}^8}. \quad \text{(A4)}$$

Substituting equation (A3) into equation (A4), with straightforward manipulation, results in

$$\tilde{\eta}_{\rm eff}(t_0) = \frac{1}{8}\{\frac{1}{t_0 V_{\rm nmo}^4(t_0)}\int_0^{t_0} v_{\rm nmo}^4(\tau)[1+8\eta(\tau)]d\tau - 1\}. \quad \text{(A5)}$$

APPENDIX B: Nonhyperbolic Moveout in Isotropic Layered Media

Typically, reflections in isotropic $v(z)$ media are approximated by hyperbolic moveout characterized by root-mean-square (rms) velocity. If the subsurface velocity has large variation in depth, the hyperbolic moveout assumption is less accurate, and an additional term in the Taylor series expansion is needed to better simulate the moveout. The three-term expansion (Taner and Koehler, 1969; Shah and Levin, 1973; Al-Chalabi, 1974) for isotropic media is given by

$$t = t_0 + \frac{X^2}{V_{\rm nmo}^2} + \frac{(1-\frac{V_4^4}{V_{\rm nmo}^4})X^4}{4t_0^2 V_{\rm nmo}^4}, \quad \text{(B1)}$$

where $V_{\rm nmo}$ is calculated using equations (7), and V_4 is calculated using the following

$$V_4^4(t_0) = \frac{1}{t_0}\int_0^{t_0} v^4(\tau)d\tau. \quad \text{(B2)}$$

The interval quantities $v_{\rm nmo}(\tau)$, and $v(\tau)$, in this case, are equal. The first two terms in equation (B1) correspond to hyperbolic moveout, and the additional term is the nonhyperbolic term, which provides better accuracy at the larger offsets. Actually, equation (3), with $\eta_{\rm eff}$ given by equation (8), reduces to equation (B1) for isotropic media.

The left portion of Figure A1 shows an isotropic $v(z)$ model consisting of three layers. The right portion shows the percent error in the computed moveout corresponding to reflections from (a) the bottom of the second layer, and (b) the bottom of the third layer. The time errors resulting from using equation (B1) [or equation (3)], given by the black curve, are overall less than those resulting from using equation (5), given by the gray curve. Both, however, are better than using a hyperbolic moveout, given by the dashed curve. Nevertheless, the difference between the two nonhyperbolic approximations is small, even for such a strong vertical inhomogeneity. This difference reduces dramatically for smoother inhomogeneity. The additional X factor in the denominator of the fourth-order term in equation (5), although extremely important for VTI models, is generally ineffective for isotropic models.

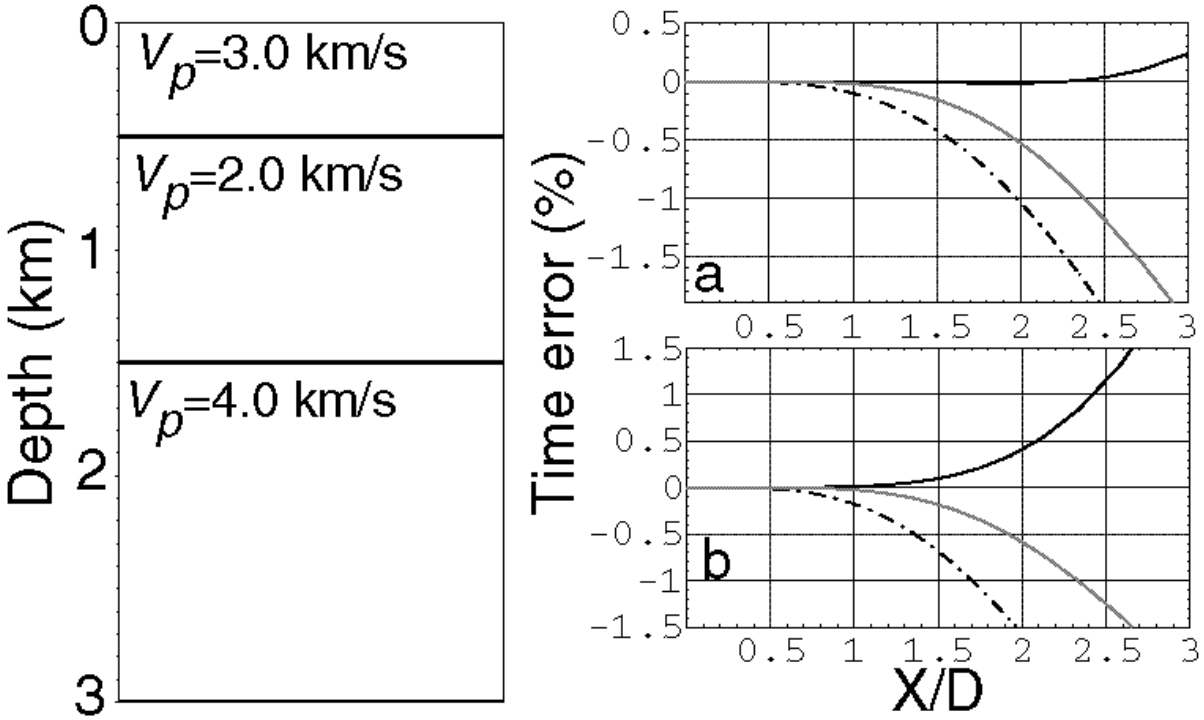

Figure A1. Left: Model with three isotropic layers. Right: Percent time error in moveout corresponding to reflections from (a) the bottom of the second layer, and (b) the bottom of the third layer. The gray curve corresponds to equation (5); the black curve corresponds to equation (3); the dashed curve corresponds to the hyperbolic moveout . V_{nmo} for all three curves is calculated using equation (7).